JOURNAL OF MATERIALS SCIENCE 28 (1993) 3014–3020

A model for lapping of glass

M. BUIJS, K. KORPEL-VAN HOUTEN
Philips Research Laboratories, P.O. Box 80.000, 5600 JA Eindhoven, The Netherlands

Lapping of glass and other brittle materials is an important economic activity. Nevertheless, it has not received much scientific attention, despite the fact that it is also related to problems of wear (three-body abrasion). Therefore, lapping of glass has been analysed in terms of the concept of lateral fracture, by studying the influence of material parameters, namely Young's modulus, hardness and fracture toughness, on material removal and surface roughness for two different sets of experimental conditions. The concept was found to be well applicable, and was therefore used to develop a model of three-body abrasion by material removal via rolling and indenting abrasives. The model gives a good description of the two experiments. It allows an average normal force per abrasive to be determined from Preston's coefficient and the characteristics of the workpiece and abrasive.

1. Introduction

The finishing of glass objects by grinding, lapping and polishing has a long-standing history. The use of glass lenses for optical experiments led scientists such as Newton [1] and Rayleigh [2] to ponder over the question as to what happens on a microscopic scale during these abrasive processes. Significant progress on this subject was made in past decades, when model experiments, focused on the interaction of single abrasive grains with the brittle workpiece surface, were performed. These experiments involved quasi-static indentations, single-point scratching, single-point grinding and multipoint grinding (for example, see [3]), very often with Vicker's diamonds. It was found that, for brittle materials like glass, a threshold exists for the normal load on the abrasive particle, below which material is removed from the workpiece surface via plastic deformation. Above this threshold, cracking occurs, which can be characterized by the terminology stemming from Vicker's indentation studies: material removal is associated with lateral cracking, whereas strength-diminishing subsurface damage is connected with radial/median cracking.

The largest effort went into exploration of the microscopic mechanisms underlying grinding (or two-body abrasion, with fixed abrasives) of brittle materials. These are now well described [4–6]. Polishing, especially of glass, has also received a fair amount of attention, very often with regard to the chemical aspects of the process [7]. Although lapping is an important abrasive finishing process, comparable to grinding and polishing of brittle materials, very little is known about it from a fundamental view point. Lapping is a three-body abrasion process in which grinding is performed with loose abrasive particles. It offers an economic advantage in large-volume processes when cheap abrasives like sand are used. It is also preferentially chosen in the case of stringent requirements concerning flatness and dimensions. Because of the importance of three-body abrasion processes for wear, most fundamental experiments on this subject have been performed with metals [8, 9]. The results can more or less be used to describe lapping of brittle materials in the ductile regime, i.e. the regime where the normal load per abrasive is below the threshold load for fracture. The boundary between this regime and polishing is diffuse. However, many lapping applications lie in the fracture regime.

The most important work on lapping of glass has been carried out by Izumitani and Suzuki [10], who found the "lapping hardness" to be a measure of resistivity to fracture by abrasive grains. They related this behaviour to indentation hardness and yield stress through Hill's theory on plastic–elastic materials. Much progress has since been made in the field of indentation theory and the application of this theory to grinding of brittle materials. The aim of the present work was to apply indentation theory also to lapping or three-body abrasion of glass. We studied the influence of glass composition, as reflected in the material parameters Young's modulus, hardness and fracture toughness, on the removal rate and surface roughness. It appears that the influence can be well described with the concept of the lateral crack. We derived a model for material removal by rolling particles, based on this concept, which was found to be in good agreement with the experimental results. The model enables the average load per particle to be calculated from Preston's coefficient, the material parameters of the workpiece and the shape and size of the abrasive.

2. Experimental procedure

2.1. Glass characteristics

The glasses used were the following optical glasses from Schott: Herasil (fused silica), ZKN 7 (crown), BK 7 (crown), LF 5 (flint), SF 55 (flint), SF 58 (flint), SF 6 (flint), F2 (flint), and standard soda–lime glass. The

0022–2461

TABLE I Glass composition (mol %) and transition temperature

	Si_2O_3	Al_2O_3	B_2O_3	PbO	BaO	ZnO	CaO	MgO	Na_2O	K_2O	T_g (°C)
1. Herasil	100										
2. BK 7	74		10		1				10	5	559
3. Soda–lime	70	1					6	6	17		550
4. ZKN 7	67	3	12			9	1		8		528
5. F 2	70			19					6	5	432
6. LF 5	72			13					9	6	419
7. SF 55	61			36						3	421
8. SF 6	57			41						1	423
9. SF 58	45		2	52							390

glasses were chosen because of their range of hardness. Their composition as determined by ICP emission is given in Table I, together with the glass transition temperature, T_g, as given by the Schott catalogue of optical glasses. All measurements were performed on samples which were annealed by heating at 3 °C min^{-1} to T_g, soaking for 10 h at that temperature and cooling to room temperature at 1 °C min^{-1}. The fused silica was annealed at 1100 °C, being the highest temperature our annealing oven could reach. The T_g of soda–lime glass was taken to be 550 °C [11].

Young's modulus, E, was determined under ambient conditions using the pulse-echo technique [12] with a longitudinal wave velocity of 5 MHz and a transverse wave velocity of 20 MHz, on samples with a diameter of 14 mm and a thickness of 3 mm, polished on both sides. The density, needed for the calculation of the modulus, was determined from the dimensions and weight of the samples. The standard deviation in the mean for the modulus determination was about 1%.

Vicker's indentations [13] with a load of 100 g were made on the same samples for the determination of the hardness, H_v, where the indentation diagonal was determined from optical micrographs. Although small radial cracks appeared at this load level, it was chosen as a compromise, involving factors like the detectability through an optical microscope, occurrence of cracks and levelling off of the load dependence of the hardness. Dwell time of the diamond was 15 s. For each value eight measurements were carried out, resulting in a standard deviation of about 5%.

Fracture toughness, K_{Ic}, was determined using the single-edge notched-bend method [14]. Twelve annealed samples per glass, measuring 15 mm × 3 mm × 1 mm, with a sawed-edge notch of 0.5 mm and a 1 kg Knoop indentation starter crack, were fractured in a three-point bending test, with a span of 12 mm and a crosshead speed of 0.1 mm min^{-1}, under ambient conditions. The standard deviation was about 10%.

2.2. Lapping

A diagram of the lapping equipment is given in Fig. 1. Three samples with a diameter of 14 mm and a thickness of 3 mm were lapped simultaneously on a rotating lapping plate (diameter 200 mm) with a spiral groove. The centre of the ring (diameter 80 mm) containing the three samples was positioned at 6 cm from the centre of the lapping plate. The lapping slurry consisted of abrasive and water in a weight ratio of 1 : 5. All samples were lapped for 40 min, starting with polished surfaces. The removal rate was determined by weighing at intervals of 4 min. It was found to be constant with time. In order to probe two different regimes with respect to removal rate, two different sets of experimental conditions were chosen. The experimental parameters were all varied in order to test the general applicability of the approach. They are given in Table II and will be referred to as "SiC/Cu" and "Al_2O_3/Sn". The nominal hardness number of the SiC and Al_2O_3 was 25 and 20 GPa, respectively. This is considerably harder than the hardest glass used in this study. To determine the dependence of removal rate on load, a series of experiments under the "SiC/Cu" conditions of Table II was performed on soda–lime glass samples, in which the load was varied from 2–16 N.

Roughness was determined on samples that had been lapped for 40 min, using a Talysurf (tip radius 2.5 μm, step size 2 μm, measured length 6.4 mm, cut-off length digital filter 800 μm).

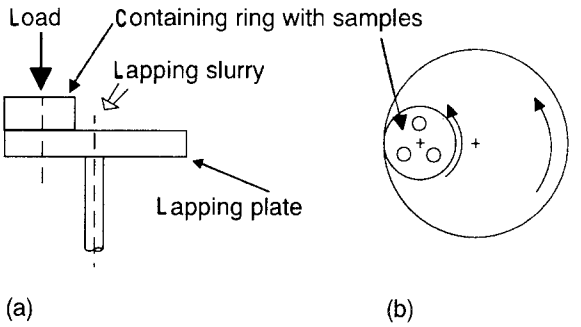

Figure 1 Schematic of lapping apparatus; (a) side view, (b) top view.

TABLE II Experimental conditions

	SiC/Cu	Al_2O_3/Sn
Lapping plate	Cu (H_v = 290 MPa)	Sn (H_v = 160 MPa)
Abrasive	150 μm SiC	22 μm Al_2O_3
Normal load (N)	5	20
Average relative velocity of lapping plate and workpiece (m s^{-1})	1.2	0.6

3. Results and discussion

3.1. Influence of material parameters

The material parameters of the glasses can be found in Table III, together with the results of the experiments. The roughness values are the R_z values, which correspond to the average peak-to-valley surface roughness.

For an interpretation of the results, it is necessary to have some idea about the behaviour of the abrasives. This can lie between two extremes: either the abrasive particles are completed embedded in the lapping plate, in which case they behave like bonded particles, or they are rolling between workpiece surface and lapping plate. The former situation is equal to two-body abrasion and can be described by models derived from scratching experiments, while the latter situation leads to an accumulation of single events in which the sharp corners of the abrasive particles indent the workpiece surface. The relative contribution of these two possibilities to the total process depends on size and shape of the abrasive particles and the relative hardness of lapping plate and workpiece surface [15].

We obtained an impression of the ratio of rolling and scratching for the two experimental conditions from optical and scanning electron micrographs of the glass surfaces taken after different periods of lapping, typically at intervals of 10 s. Figs 2 and 3 give examples of such micrographs. Lapping with the copper plate resulted for all glasses in indentation craters due to rolling abrasives. Only a few scratches due to embedded particles could be observed. Lapping with the tin plate gave rise to many more scratches, comparable to the amount of craters. This is in accordance with the relative hardness of the two plates. As can be seen in Figs 2 and 3, for both sets of experimental conditions most craters were accompanied by conchoidal fracture, which is characteristic of lateral chipping [16, 17]. In the literature, there is some discussion on whether this type of fracture should be classified as the "standard" subsurface lateral crack which is known from Vicker's indentations, or whether it is the so-called shallow lateral crack, which seems to originate from secondary radial cracks [18, 19]. As little is known about the latter, we treated all cracks as resulting from subsurface lateral fracture.

It is surprising that in the Al_2O_3/Sn experiments, the single-indentation events lead to fracture while the scratching does not. It is known that the presence of a tangential load, such as during scratching, leads to a lowering of the fracture threshold [20]. For instance, Srinivasan and Scattergood [16] observed the chipping probability of window glass eroded by solid particles to be higher for oblique incidence than for normal incidence. In our experiments, it would then appear that the tangential load which acts on the rolling particle is greater than the tangential load on the scratching particle.

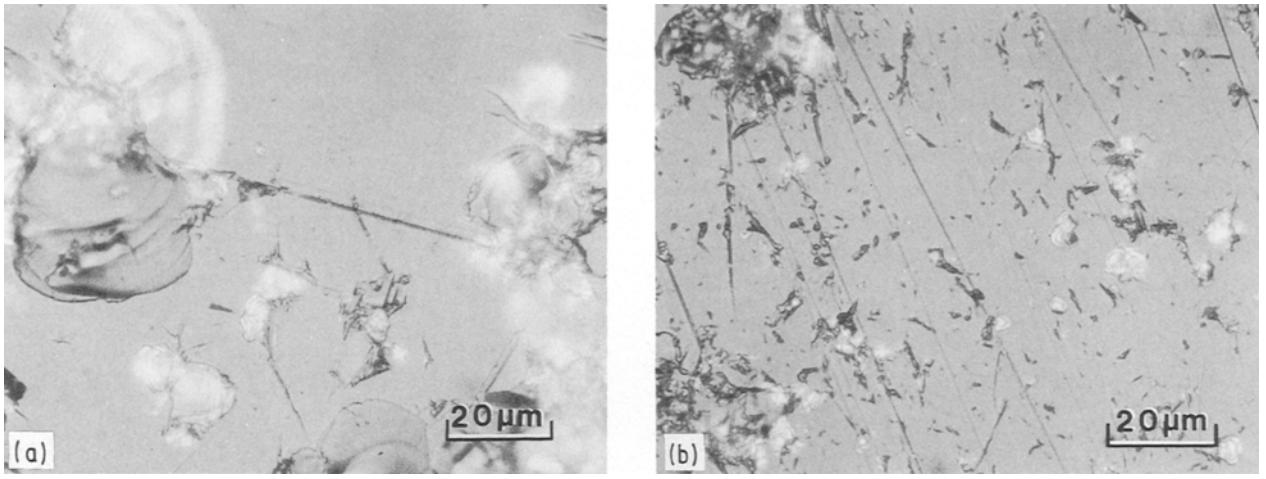

Figure 2 Optical micrograph of soda–lime glass surface, lapped for 10 s, (a) SiC/Cu, (b) Al_2O_3/Sn.

TABLE III Glass parameters and lapping results

	E (GPa)	H_v (GPa)	K_{Ic} (MPa $m^{1/2}$)	Removal rate (nm s^{-1})		Surface roughness (µm)	
				SiC/Cu	Al_2O_3/Sn	SiC/Cu	Al_2O_3
1. Herasil	71.8	7.1	0.70	222	148	12.2	3.48
2. BK 7	79.9	5.9	0.83	502	212	13.7	3.49
3. Soda–lime	72.0	5.4	0.85	458	194	14.1	3.95
4. ZKN 7	69.0	5.4	0.71	302	149	14.3	2.15
5. F 2	56.4	4.6	0.55	708	310	15.8	4.87
6. LF 5	58.3	4.3	0.61	677	281	15.4	3.60
7. SF 55	56.1	4.1	0.49	1190	465	13.1	4.66
8. SF 6	54.7	3.7	0.54	1220	527	16.0	5.73
9. SF 58	49.3	3.1	0.38	2080	878	20.2	5.61

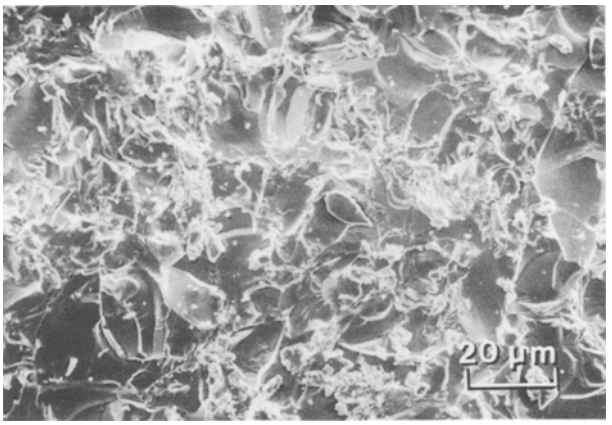

Figure 3 Scanning electron micrograph of soda–lime glass surface, lapped for 20 s (SiC/Cu).

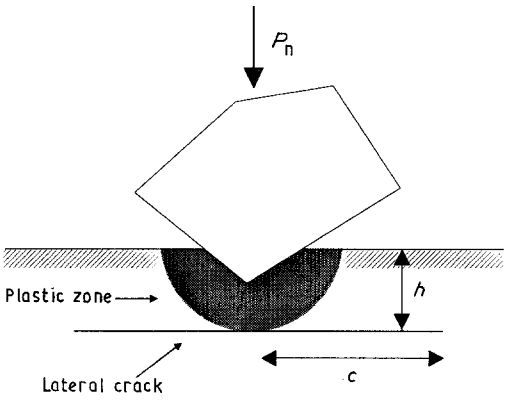

Figure 4 Schematic representation of an indentation event.

The scratching as observed on the micrographs removes material via ploughing and plastic deformation. This process is ten times less effective than material removal by fracture in terms of specific energy [4, 21]. It therefore seems reasonable to assume that the three-body abrasion in our Al_2O_3/Sn experiments is also dominated by the indentation events of the rolling particles. The basis for the modelling will thus be the lateral crack, which has been extensively studied in quasistatic indentation experiments. Material removal occurs either by chipping of a lateral crack, which requires only one indentation, or by coalescence of multiple unchipped lateral cracks. Although the presence of a tangential load enhances the lateral crack extension, a quasi-static approach was found to lead to good results [16]. The indentation of a sharp particle will deform the workpiece surface elastoplastically, producing a plastic zone with residual tensile stresses which generate and propagate the lateral crack. This is shown schematically in Fig. 4. According to Marshall *et al.* [22], the equilibrium length, c, of the lateral crack is given by

$$c = \alpha_0 \frac{E^{3/8}}{K_{Ic}^{1/2} H^{1/2}} P_i^{5/8} \quad (1)$$

where α_0 is a material-independent constant which depends on particle shape; E, H and K_{Ic} refer to the brittle workpiece and P_i is the normal load on the particle.

Although there is a distribution of lateral crack sizes in both sets of experiments, it can be said that the cracks are larger in the SiC/Cu experiment than in the Al_2O_3/Sn experiment. For the soda–lime glass samples of Figs 2 and 3, they are of the order of 10 and 1 μm, respectively, as determined from micrographs of craters and glass debris. From these values an estimate of the order of the normal load per particle for the two experimental conditions can be derived from Equation 1. For clarity and simplicity we will neglect distributions and assume that the whole process can be described in terms of average particle size, particle shape and normal load per particle. Scanning electron micrographs of the abrasive particles show that the SiC particles are blunter than the Al_2O_3 particles. An estimate for the angle of the indenting points of the particles could be obtained from the scanning electron micrographs. The SiC particles have angles close to the angle of the Vicker's indentor (140°), while those of the Al_2O_3 particles are approaching 90°. This can be used to calculate α_0 in Equation 1 [22] to be 0.12 and 0.17, respectively, resulting in an average normal load per particle of 0.4 and 0.005 N, respectively. This indicates two orders of magnitude difference in normal load per particle between the two experimental conditions.

Lateral cracks originate from the bottom of the plastic zone. Their depth, h, is given by [22]

$$h = \alpha_1 \frac{E^{1/2}}{H} P_i^{1/2} \quad (2)$$

where α_1 is another constant which depends on the particle shape.

The volume, V_i, of workpiece material removed per indentation event above the fracture threshold is

$$V_i = \pi c^2 h \quad (3)$$

Substituting Equations 1 and 2 into Equation 3, this becomes

$$V_i = \alpha_2 \frac{E^{5/4}}{K_{Ic} H^2} P_i^{7/4} \quad (4)$$

The total removal rate, Z, consists of the sum over all indentation events i. Because the material parameters E, H and K_{Ic} are independent of i, Z should be linearly dependent on $E^{5/4}/(K_{Ic}H^2)$. Plotting the data of Table III accordingly in Fig. 5 shows that this is indeed the case. The model of lateral fracture, as developed for quasi-static Vicker's indentation experiments, is therefore well suited to describe the material removal for this regime of three-body abrasion. One should not, however, attach too much significance to the exact value of the exponents in Equation 4. More important is the fact that Z does not scale with H^{-1}: this clearly distinguishes this regime from the purely ductile regime [21].

From Fig. 4, it appears that the roughness induced by a three-body abrasion process, consisting of separate indentation events is related to the depth of lateral cracking. The resulting linear dependence of roughness on $E^{1/2}/H$, as following from Equation 2, is shown in Fig. 6. From the values for the indenting

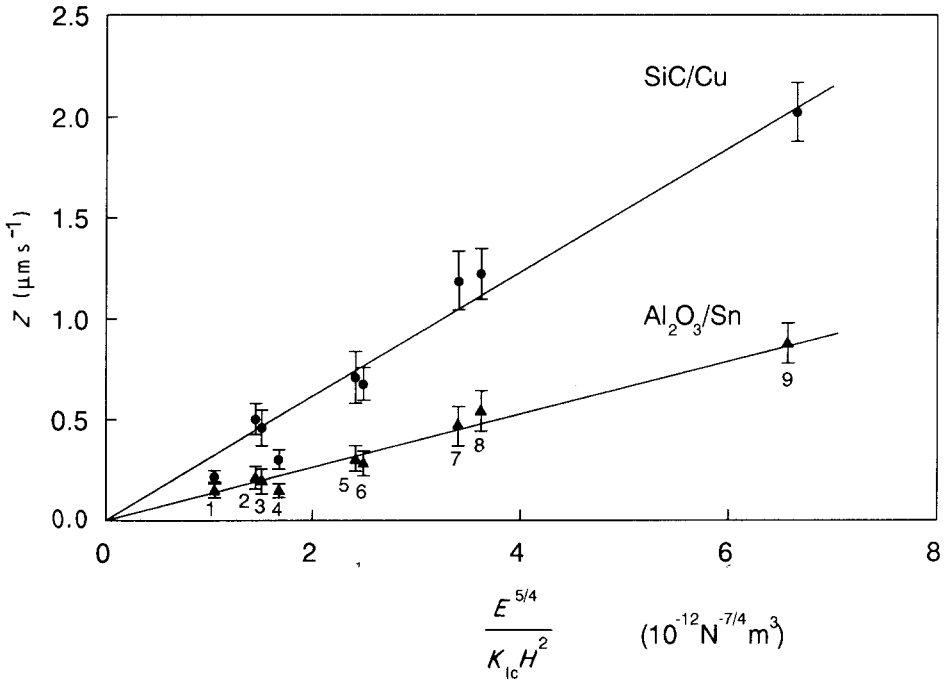

Figure 5 Removal rate, Z, as a function of E, K_{Ic} and H, according to Equation 4; (—) constrained linear fit; numbering refers to Table III.

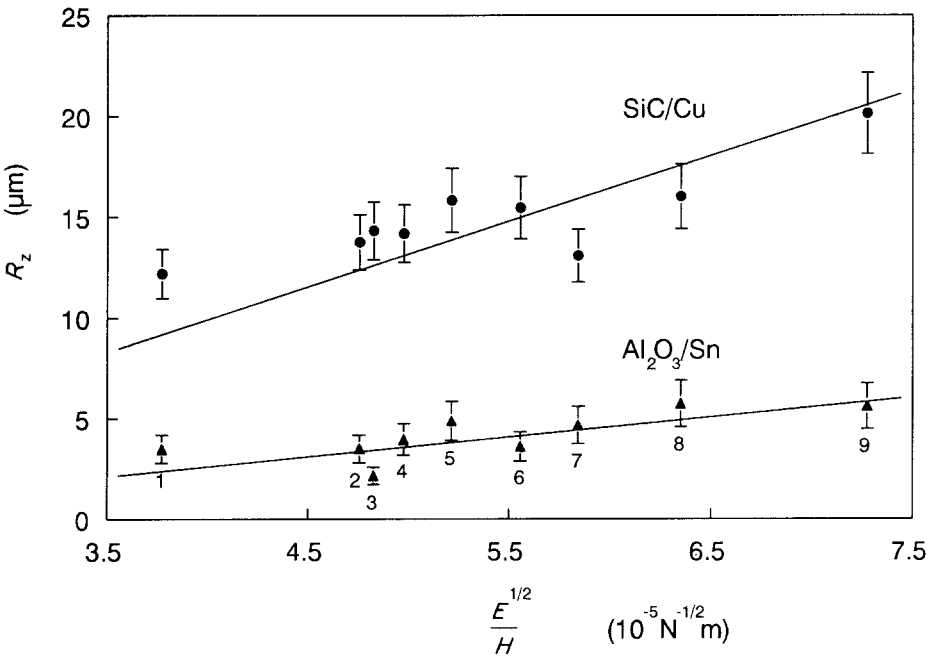

Figure 6 Roughness, R_z, as a function of E and H, according to Equation 2; (—) constrained linear fit.

angles of SiC and Al_2O_3, α_1 can be calculated to be 0.52 and 0.71, respectively [22]. The slope of the least-squares fit (constrained to intercept = 0) in Fig. 6 should be equal to $\alpha_1 P_i^{1/2}$. This results in values for P_i of 0.3 and 0.01 N, respectively. The order of magnitude agrees with that derived from the micrographs. Differences may be due to overlap of fractures. This will not, however, influence the dependence on material parameters.

3.2. Lapping model

A model for the description of three-body abrasion is now developed, based on the integration of the lateral fracture concept with an earlier model for loose-abrasive grinding by Wiese and Wagner [23]. It starts from the assumption that material removal occurs by rolling particles, that at all times M abrasive particles (not necessarily always the same) are in simultaneous contact with lapping plate and workpiece, and that they are uniformly distributed over the workpiece area, A_{wp}. This area can then be divided into segments of area A_{seg}, with $A_{wp} = MA_{seg}$. Each segment will, on average, contain one abrasive. This is illustrated in Fig. 7. The load per abrasive, P_i, is given by the total load, P_{tot}, divided by M. When P_i is larger than the fracture threshold, a lateral crack will be introduced in the segment, with an effective area A_{cell}. Each segment

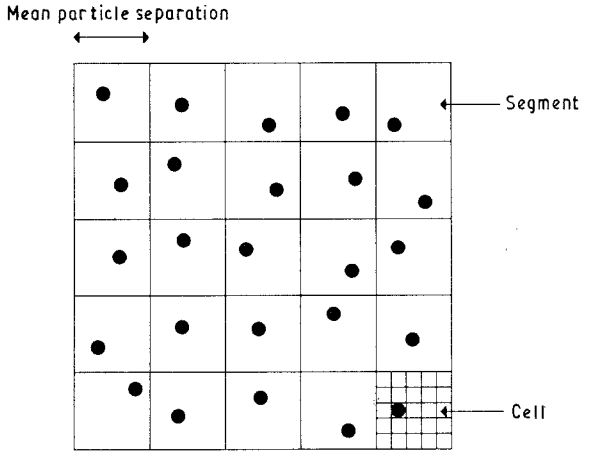

Figure 7 Idealized view of workpiece surface, divided in segments and cells; (●) abrasive particles.

can be subdivided into N cells of area A_{cell}. As the abrasion progresses and the particles roll between plate and workpiece, each segment continues to contain one particle on average, but with a shifting position with respect to the cells of a segment. So a succession of cracks will appear in the segment.

Assume that, after time t during abrasion, $n(t)$ cracks are formed per segment, with $m(t)$ cells per segment covered by cracks. The fraction of cells covered by cracks in any one segment is $E\{m\}/N$, where $E\{m\}$ is the expectation value of the average number $m(t)$ per segment. In a previous study, we have shown that lateral cracks in glass do not interact [24]. Material will then be removed when the load is high enough for chipping, or when an unchipped lateral crack is surrounded by other lateral cracks. The average volume, V, of material removed in a segment by a fracturing indentation is $V = V_i(E\{m\}/N)^x$, where x depends on the number of coalescing lateral cracks needed for one lateral crack to be removed. V_i is given by Equation 4. With dn cracks occurring in a time interval dt, the total depth, $h(t)$, removed per segment after time t is given by

$$h(t) = \int_0^{n(t)} \frac{V_i}{A_{seg}} \left(\frac{E\{m\}}{N}\right)^x dn \quad (5)$$

The indenting frequency of an abrasive particle is determined by the relative velocity, v, of the lapping plate with respect to the workpiece and the mean radius, R, of the rolling particles. This results in the following expression for dn

$$dn = \alpha_3 \frac{v}{2\pi R} dt \quad (6)$$

where α_3 depends on particle shape. Combining Equations 5 and 6 leads to an expression for the removal rate $Z = dh/dt$

$$Z(t) = \alpha_3 \frac{V_i}{A_{seg}} \left(\frac{E\{m\}}{N}\right)^x \frac{v}{2\pi R} \quad (7)$$

Equation 7 can be simplified by considering that Z is independent of time under steady-state abrasion conditions. In that case the density of lateral cracks is so high that every new crack will lead to material removal. This means that x in Equation 7 can be taken to be zero. Using Equations 4–6 and the fact that $A_{seg} = A_{wp}(P_i/P_{tot})$, Equation 7 becomes

$$Z = \alpha_4 \frac{v P_i^{3/4} P_{tot}}{R A_{wp}} \frac{E^{5/4}}{K_{Ic} H^2} \quad (8)$$

where $\alpha_4 = \alpha_0^2 \alpha_1 \alpha_3/2$, or

$$Z = \beta \frac{E^{5/4}}{K_{Ic} H^2} \quad (9)$$

The factor β is the slope of the lines in Fig. 5. Because v, P_{tot}, R and A_{wp} are known, we can use β to calculate P_i for the two sets of experiments. Taking $\alpha_3 = 1$ as an estimate from [23], this results in average normal loads per particle of 0.5 and 0.001 N, respectively. In view of the assumptions made, this compares favourably to the 0.4 and 0.005 N deduced from the micrographs. It is interesting to note that P_i for Al_2O_3/Sn becomes 0.003 N when P_{tot} is taken to be 10 N instead of 20 N, which would be the total load experienced by the rolling abrasives when an equal number of embedded abrasives is scratching the workpiece surface at the same time. This indicates that the exact fraction of rolling abrasives is of minor importance. It appears from these results that for SiC/Cu, about 10 abrasives are in simultaneous contact with lapping plate and workpiece, while 4 000–20 000 abrasives are active for Al_2O_3/Sn.

The value of the model for the description of three-body abrasion is apparent, considering the fact that the two experiments differ in so many parameters: load, velocity, shape and size of abrasives and hardness of lapping plate. Equation 8 agrees with the well-known relation found by Preston [25], who showed that the removal rate is proportional to the total pressure multiplied by the relative velocity of abrasion tool and workpiece. In agreement with Equation 8 we found the removal rate to be proportional to the total load. Equation 8 is well suited to derive P_i, which is characteristic for the lapping plate–abrasive–workpiece interaction, from the experimentally determined Preston's coefficient, the properties of the workpiece and the shape of the abrasives. Finally, it should be noted that this model can also be applied to other brittle materials, as long as their material properties are characterized by E, H and K_{Ic}.

In conclusion, it was shown that lapping or three-body abrasion of glass can be accurately described with the concept of lateral fracture, which originates from quasi-static Vicker's indentation experiments. This was done by examining the influence of the material parameters Young's modulus, hardness and fracture toughness on removal rate and surface roughness. A model for the description of lapping is proposed, based on this concept and the notion of material removal by rolling abrasives. The model was found to describe the experiments very well. It allows the average normal load per abrasive to be determined from Preston's coefficient and workpiece and abrasive properties.

Acknowledgements

We thank Mr Horden and Mr Alting for the preparation of the samples, Mr Nulens for the measurement of the roughness, and Mrs Baeten for the determination of the composition of the glasses.

References

1. R. P. FEYNMAN, "QED, the Strange Theory of Light and Matter" (Princeton University Press, Princeton, NJ, 1985).
2. LORD RAYLEIGH, *Proc. Roy. Inst.* **16** (1901) 563.
3. D. B. MARSHALL, A. G. EVANS, B. T. KHURI YAKUB, J. W. TIEN and G. S. KINO, *Proc. Roy. Soc. (Lond.)* **A385** (1983) 461.
4. A. BROESE VAN GROENOU and J. D. B. VELDKAMP, *Philips Tech. Rev.* **38** (1978/79) 105.
5. H. P. KIRCHNER, *J. Amer. Ceram. Soc.* **67** (1984) 347.
6. P. MOLLOY, M. G. SCHINKER, and W. DOLL, *SPIE* **802** (1987) 81.
7. L. M. COOK, *J. Non-Cryst. Solids* **120** (1990) 152.
8. E. RABINOWICZ, L. A. DUNN and P. G. RUSSELL, *Wear* **4** (1961) 345.
9. L. FANG, Q. D. ZHOU and Y. J. LI, *ibid.* **151** (1991) 313.
10. T. IZUMITANI and I. SUZUKI, *Glass Technol.* **14** (1973) 35.
11. H. SCHOLZE, "Glas, Natur, Struktur und Eigenschaften" (Springer, Berlin, 1988) p. 42.
12. H. F. POLLARD, "Sound Waves in Solids" (Pion, London, 1977).
13. R. F. COOK and D. H. ROACH, *J. Mater. Res.* **1** (1986) 589.
14. J. E. SRAWLEY and B. GROSS, in "Cracks and Fracture" edited by G. L. Swedlow and M. L. Williams, ASTM STP **601** (American Society for Testing and Materials, Philadelphia, PA, 1976) p. 559.
15. J. A. WILLIAMS and A. M. HYNCICA, *Wear* **152** (1992) 57.
16. S. SRINIVASAN and R. O. SCATTERGOOD, *J. Mater. Sci.* **22** (1987) 3463.
17. L. MURUGESH and R. O. SCATTERGOOD, *ibid.* **26** (1991) 5456.
18. R. F. COOK and G. M. PHARR, *J. Amer. Ceram. Soc.* **73** (1990) 787.
19. R. F. COOK, M. R. PASCUCCI and W. H. RHODES, *ibid.* **73** (1990) 1873.
20. S. S. CHIANG and A. G. EVANS, *ibid.* **66** (1983) 4.
21. M. A. MOORE and F. S. KING, *Wear* **60** (1980) 123.
22. D. B. MARSHALL, B. R. LAWN, and A. G. EVANS, *J. Amer. Ceram. Soc.* **65** (1982) 561.
23. G. E. WIESE and R. E. WAGNER, *Appl. Opt.* **13** (1974) 2719.
24. M. BUIJS and E. A. A. MARTENS, *J. Amer. Ceram. Soc.*, **75** (1992) 2809.
25. F. W. PRESTON, *J. Glass Technol.* **11** (1927) 214.

Received 10 April
and accepted 19 October 1992